

ISTITUTO NAZIONALE DI FISICA NUCLEARE
Laboratori Nazionali di Frascati

LNF-86/25(NT)
4 Luglio 1986

A. Balerna, S. Mobilio and A. Merlini:
EXAFS IN A DISPERSIVE MODE. I: THEORY AND PERFORMANCES
OF CYLINDRICALLY BENT CRYSTALS

EXAFS IN A DISPERSIVE MODE.

I : Theory and performances of cylindrically bent crystals

A. Balerna and S. Mobilio

INFN-Laboratori Nazionali di Frascati-C.P.13-00044 Frascati-ITALY

A. Merlini

Divisione di Fisica - CCR EURATOM- 21020 Ispra (Va)-ITALY

1. - INTRODUCTION

In the last ten years the Extended X-ray Absorption Fine Structure (EXAFS) spectroscopy has been developed as an effective tool to determine the local structure around the absorbing atom in a great variety of materials like amorphous metals and semiconductors, glasses, catalysts, solutions, biological systems and so on^(1,2).

During this time the sensitivity of the original transmission experimental technique has been increased by measuring the X-ray absorption coefficient through the detection of secondary processes which follow the primary photo-absorption. Monitoring, for example, the X-ray fluorescence, dilute systems in the sub-millimolar range can be studied. Monitoring the Auger and/or photoemission secondary electrons, adsorbates and surfaces can be investigated in the existing synchrotron radiation (S.R.) facilities^(3,4).

The present interest is the development of experimental apparatus which allow to perform time resolved EXAFS studies to monitor dynamical processes like chemical reactions on surfaces or enzymatic reactions.

Such studies cannot be realized with the standard EXAFS experimental apparatus, which implies data collection by scanning the X-ray monochromator in small steps in the energy range of interest.

Therefore a new experimental approach has been developed : it is an energy-dispersive method which allows the collection of the whole spectrum simultaneously, thus shortening the acquisition time from minutes up to seconds (dispersive mode)^(5,6).

With the advent of new wigglers and future planned X-ray machines, a time scale lower than the millisecond will be reached if new fast position sensitive X-ray detectors will be developed as well.

A dispersive EXAFS apparatus can be realized by dispersing the quasi-parallel X-ray beam coming from the electron storage ring by means of a cylindrically bent crystal (fig. 1). Since the incident angle of the primary X-ray beam varies continuously along the crystal surface, different X-ray energies will be reflected from different points on the crystal surface. The energy dispersed beam converges to a focus at the sample position. The beam transmitted through the sample then diverges towards a position sensitive detector or a film.

In this report we describe the theory, characteristics and performances of cylindrically bent crystals applied to Synchrotron Radiation sources. We also describe a prototype system designed and realized in collaboration with the Physics Division of the EURATOM in Ispra. This is the first step of a project to build up a dispersive EXAFS experimental facility in the Frascati S.R. Laboratories .

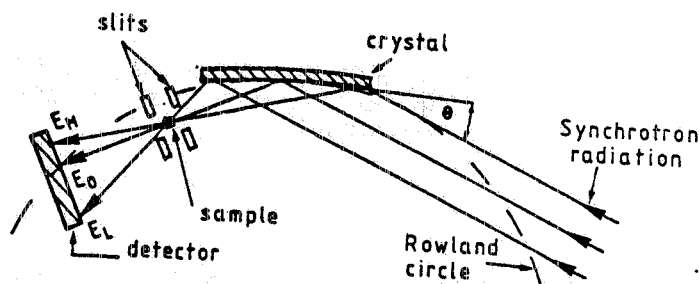


FIG.1 - Geometrical arrangement of a dispersive X-ray spectrometer.

2. - CYLINDRICALLY BENT CRYSTALS : THEORY

a. - Focus position

As in the usual Rowland theory of diffracting gratings the best focus condition of a cylindrically bent crystal is given by the relation⁽⁷⁾:

$$\sin^2 \alpha / r - \sin \alpha / R + \sin^2 \beta / r' - \sin \beta / R = 0$$

where R is the radius of curvature of the crystal, r and r' are the absolute values of the source to crystal and crystal to focus distances and α and β are the angles between the crystal surface and the source to crystal and focus to crystal directions respectively. For a Bragg type reflection on a symmetric-cut crystal since $\alpha = \beta = \theta_0$ the focus condition becomes:

$$1/r + 1/r' = 2/R \sin \theta_0 \quad (1).$$

This equation has different solutions. The Rowland geometry uses the symmetric solution of such equation, $r = r' = R \sin \theta_0$. It describes the situation in which both the source and the image are on a circle of radius $R/2$ tangent to crystal surface (Rowland circle) (fig. 2).

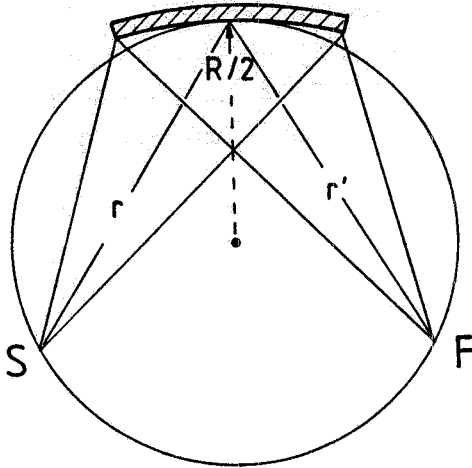


FIG.2 -- The Rowland geometry: the source and its image are both on a circle of radius $R/2$ in symmetric positions.

From eq. 1 it is clear that when the source is located outside the Rowland circle, the focal point will be within the circle (fig.1).

In the case of S.R. we can let $r \rightarrow \infty$, so the focal point is given by $r' = R \sin \theta_0 / 2$.

b. - Horizontal focal dimensions

At the focal point the source will be imaged in a vertical line whose horizontal dimension, h , is ideally given by $(h_s r')/r$, h_s being the source horizontal dimension and r'/r the demagnification of the optical system. Two effects contribute to enlarge this horizontal focus dimension. The first is due to the aberrations of the optical system whose contribution, h_A , is of the order of $h_A = L^2/BR$ where L is the crystal length. The second one, $h_{i,n}$, is due to the intrinsic angular dispersion of the diffracted X-ray beam (Darwin width) and is given by:

$$h_{in} = \omega r'$$

Considering these three contributions, the total horizontal width at the focus, h_T , will be given by:

$$h_T = h_{sr}'/r + L^2/8R + \omega r' \quad (2).$$

c. - Dispersive properties

The peculiarity of the dispersive EXAFS approach is that the whole spectrum can be recorded simultaneously; this is possible only if for a fixed crystal position a wide energy range ($\Delta E = 800\text{eV} - 1000\text{eV}$) is obtainable. It is evident from Fig. 3a that the different X-ray paths which reach the crystal, hit its surface at different angles and are also reflected at different wavelengths.

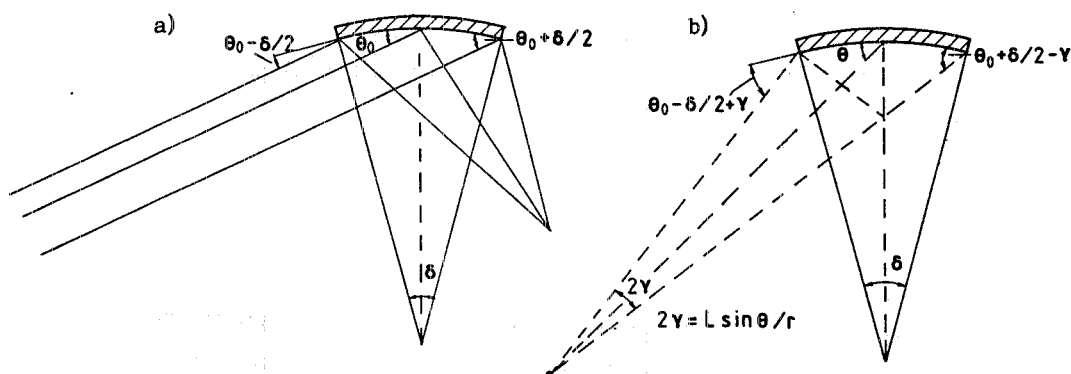


FIG.3 - a) Origin of the angular spread in the glancing angle for a parallel incoming X-ray beam; the angular spread is due to the angular opening, δ , of the curved crystal; b) the same as Fig. 3a considering a point source. In this geometry the divergence of the incoming beam must be subtracted to the angular opening of the crystal.

If, δ , is the total angular acceptance of the crystal then the full energy range ΔE is given by the derivative of the Bragg law:

$$\Delta E = E_0 \cotg \theta_0 \delta$$

θ_0 and E_0 being the glancing angle and the energy of the middle path respectively.

For a point source, at a finite distance, the angular spread due to the incident angle is $\delta' = (L'/R - L' \sin \theta_0 / r)$ (fig. 3b) and the energy range is:

$$\Delta E = E_0 \cotg \theta_0 (L'/R - L' \sin \theta_0 / r) = E_0 \cotg \theta_0 (L'/R) (1 - R \sin \theta_0 / r) \quad (3)$$

where L' is the crystal length effectively illuminated by the X-ray beam.

In some cases, when the source horizontal divergence limits the glancing angle, it is more useful to express the energy range covered in terms of the horizontal divergence of the X-ray source, Δ_h . Since, in this case, the effective crystal length illuminated is :

$$L' = \Delta_h r / \sin \theta_0,$$

ΔE can be expressed as:

$$\Delta E = E_0 \cot \theta_0 \Delta_h \left\{ \left(\frac{r}{R \sin \theta_0} \right) - 1 \right\} \quad (3')$$

If the source has a non negligible horizontal dimension, h_s , also the angular spread, h_s/r , must be taken into account, besides, of course, the intrinsic angular spread of the X-ray reflection given by the width of the rocking curve ω . The total energy range is so given by:

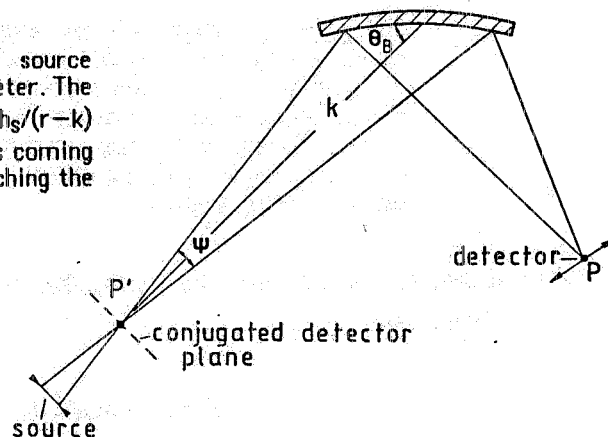
$$\Delta E = E_0 \cot \theta_0 \left\{ \left(\frac{L'}{R} - \frac{L' \sin \theta_0}{2} \right)^2 + \left(\frac{h_s}{r} \right)^2 + \omega^2 \right\}^{1/2}.$$

Anyhow in all practical cases the corrections due to the last two effects are negligible so eq. (3) and eq. (3') can be used.

d. - Energy resolution

Three different factors contribute to the energy resolution of this kind of spectrometer. The first one is the size of the X-ray source. Referring to Fig. 4 two X-ray paths coming from

FIG.4 - Contribution of the horizontal source dimension to the resolution of the spectrometer. The resolution is given by eq. (3') with $\Delta_h = h_s/(r-k)$ being the horizontal divergence of the paths coming from different points on the source and reaching the same detector point.



different source points and hitting the detector at the same point P must pass through the conjugated point P'. At P' the full beam divergence is given by $h_s/(r-k)$ where k is the distance between P' and the crystal. The angular spread of the incident angles becomes $h_s/(r-k) \{1 - k/R \sin \theta_0\}$ and the correspondent energy contribution is:

$$\delta E_1 = h\nu / (r-k) \{ k/R \sin \theta_0 - 1 \} E_0 \cot \theta_0 \quad (4).$$

Note how this contribution is minimized when $k=R \sin \theta_0$; from eq. 1 it is clear that the detector and its image are both on the Rowland circle at the same distance D from the crystal.

The second contribution is due to the intrinsic resolution of the crystal which contributes as:

$$\delta E_2 = \omega E_0 \cot \theta_0 \quad (5).$$

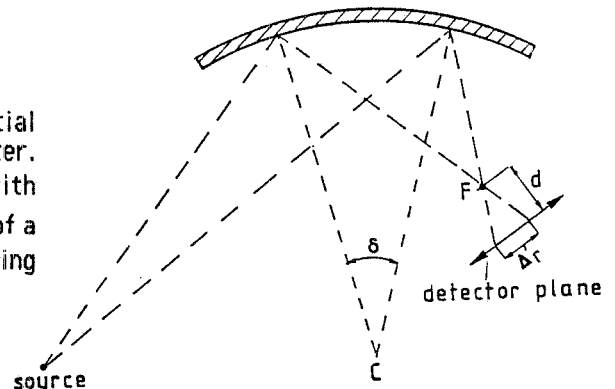
The third one is due to the spatial resolution Δr of the detector. Supposing a distance d from the focus to the detector the contribution to the energy resolution is (fig. 5):

$$\delta E_3 = \Delta r / d \{ (1/R - \sin \theta_0 / r) / (2/R - \sin \theta_0 / r) \} E_0 \cot \theta_0 \quad (6).$$

The total energy resolution δE_T is then given by:

$$\delta E_T = (\delta E_1^2 + \delta E_2^2 + \delta E_3^2)^{1/2} \quad (7).$$

FIG.5 - Contribution of the detector spatial resolution to the resolution of the spectrometer. Again the resolution is given by eq. (3'), with $\Delta_h = (\Delta r / d)(r' / r)$ being the horizontal divergence of a point source at r , focussed at r' with an image having an angular divergence $\Delta r / d$.



3. -CYLINDRICALLY BENT CRYSTALS: PERFORMANCES ON THE FRASCATI S.R. SOURCES

At the moment at the Frascati S.R. Laboratories, two X-ray beam lines are available^(8,9); the first one makes use of the S.R. coming from the bending magnet (PULS X-ray beam line), the second of the S.R. produced by a 6 pole wiggler magnet (PWA X-ray beam line-BX1). The characteristics of these two beam lines are reported in Table 1a.

The other relevant parameters in the evaluation of the performances of cylindrically bent crystals as spectrometers for dispersive EXAFS measurements are the source to crystal distance (r), the available crystal to detector distance (D) and the detector spatial resolution

(Δr). Table 1b reports possible values of such parameters. The source to crystal distances have been chosen as the minimum possible value, that means with the crystal positioned as near as possible to the Be window in the PULS and PWA laboratories. The crystal to detector distance has been fixed to 1m in order to match the space available in the existing cages. The detector spatial resolution is the one nowadays obtainable from commercial position sensitive detectors.

TAB.1 - a) The PULS and PWA source characteristics; b) possible values of the relevant geometrical arrangements of the dispersive spectrometer.

a)

BEAM LINES PARAMETERS	PULS	PWA
σ_x (mm)	1.06	1.63
$\sigma_{x'}$ (mrad)	0.25	0.16
h_s (mm)	2.12	11.50
\int_c (A)	8.26	4.50
Be _w (mm)	12.5 (circular)	10 (V)x20 (H)
Δ_h (mrad)	0.76	0.66
B _o (kGauss)	10.0	18.5
R _m (m)	5.0	2.7

b)

BEAM LINES SPECTR. PARAMETERS	PULS	PWA
r (m)	18.1	32.0
D (m)	1.0	1.0
R (m)	3.0	3.0
Δr (μ m)	25	25

Table 2 reports the calculated values of the position (r') and horizontal dimension (h) of the focus, the spectral range (ΔE) and the energy resolution (δE) at different energies obtained considering 100mm long Si(111) and Si(220) crystals and assuming a radius of curvature of 3m. On the PULS beam line the use of a Si(111) crystal allows to obtain energy ranges and resolutions good enough for EXAFS measurements at all available energies greater than 6keV, while the use of a Si(220) crystal allows rapid and high resolution XANES studies to be performed.

TAB. 2 - Performances of the dispersive spectrometer using the PULS and PWA X-ray sources, Si(111) or Si(220) as curved crystals with a fixed radius of curvature R=3 m and a crystal-detector distance of 1 m.

PULS													PWA													
Si (111)													Si (111)													
CRYSTAL	4	6	9	12	14	4	6	9	12	14	4	6	9	12	14	CRYSTAL	4	6	9	12	14					
ENERGY (keV)	762	507	335	250	214	758	501	332	248	213	758	501	332	248	213	Si(220)	1298	845	555	413	353	1259	828	548	409	350
r' (mm)	.53	.49	.47	.46	.45	.72	.61	.55	.51	.50	.90	.74	.63	.57	.55	h (mm)	.60	.55	.50	.48	.47	.90	.74	.63	.57	.55
ΔE (eV)	66	240	837	2005	3193	96	357	1259	3031	4338	24	117	445	1095	1763	ΔE (eV)	13	66	255	635	1025	24	117	445	1095	1763
δE (eV)	.39	.44	.75	1.20	1.86	.53	.80	1.20	1.60	1.86	.22	.34	.50	.67	.78	δE (eV)	.22	.34	.50	.67	.78	.22	.34	.50	.67	.78
δE (eV)	.91	.03	1.23	1.93	4.24	.36	.43	.75	1.20	1.56	-	.68	.65	.91	1.13	δE (eV)	-	.78	.70	.92	1.14	-	.68	.65	.91	1.13
δE (eV)	1.12	.91	1.89	2.78	4.89	2.74	.91	3.99	9.00	13.23	4.36	6.14	.72	2.53	3.54	δE (eV)	1.17	2.25	.24	.84	1.17	4.36	6.14	.72	2.53	3.54
ph/φ · pix	8.6x10 ³	4.1x10 ⁷	4.4x10 ⁶	5.3x10 ⁵	1.9x10 ⁵	2.6x10 ⁹	1.1x10 ⁸	6.6x10 ⁷	3.1x10 ⁷	1.6x10 ⁷	2.6x10 ⁹	1.1x10 ⁸	6.6x10 ⁷	3.1x10 ⁷	1.6x10 ⁷	ph/φ · pix	-	5.8x10 ³	5.6x10 ⁶	5.4x10 ⁵	1.5x10 ⁵	-	3.6x10 ³	4.4x10 ⁷	2.0x10 ⁷	8.6x10 ⁶

On the wiggler beam line, on the other hand, the energy resolution is worst essentially due to the higher source horizontal dimensions. In the geometrical arrangement chosen, a reasonable resolution at photon energies greater than 9 keV can be reached only by using a Si(220) crystal. The best approach would be to change the radius of curvature of the crystal to minimize the source horizontal width contribution to the resolution imposing $k=R\sin\theta$. Table 3 reports the R values to use in such situation. In this case the source horizontal width does not play any role. Since the source to crystal distance is so high that it is possible to neglect the value $1/r$ with respect to $1/r'$, it follows from eq.(1) that the crystal to focus distance is fixed at a value equal to $D/2$ for all possible energies. The new spectrometer performances for both the PULS and PWA beam lines are reported in Table 3.

Intensities obtainable at different energies have been calculated and are reported in Table 2. Typical intensities between 10^6-10^8 photons/(s.pixel) for 100mA can be achieved, giving the possibility to measure high quality absorption spectra in acquisition times ranging from 10^{-2} s up to 1s.

4. - DISPERSIVE EXAFS: CRYSTAL BENDING SYSTEM

Figs. 6 and 7 show two views of the crystal holder realized to perform dispersive EXAFS measurements.

As shown in fig. 2 the crystal has a triangular shape with an height of 100mm and a base of 30mm. The crystal thickness is of 0.5mm. The triangular shape has been chosen because a constant curvature is required. In fact for small deflections, in a triangular geometry, the curvature (c) is at any point proportional to the external bending force (F):

$$c=kF$$

where k is a constant.

Since the curvature doesn't depend on the application point of the external force, it turns out that for a triangular geometry the curvature is constant along the crystal surface. This triangular crystal is supported by an holder which fixes its base leaving the apex free to move (fig. 7). To curve the crystal the apex is translated by using a micrometer adjustment which moves a spring loaded ball race which ensures a frictionless contact to the crystal. The curvature of the crystal depends on the apex movement, x, by the relation:

$$x=L^2/2R$$

The crystal holder is fixed at a rotating stage which allows to orient horizontally the crystal, with its base perpendicular to the X-ray beam. Two more translational movements are possible in the directions of the X and Y axes in the horizontal plane to center the beam on the crystal surface.

TABLE 3 - The same as table 2, with a radius of curvature R varying according to $R=D/\sin \theta$. In such geometry the image point is at $r=D/r$ at any energy.

		PULS												PWA											
CRYSTAL		Si (111)						Si (111)						Si (220)						Si (220)					
ENERGY (keV)		4	6	9	12	14	14	4	6	9	12	14	14	4	6	9	12	14	14	4	6	9	12	14	
R (m)		2.0	3.0	4.5	6.0	7.0	7.0	2.0	3.0	4.5	6.0	6.0	7.0	2.0	3.0	4.5	6.0	6.0	7.0	2.0	3.0	4.5	6.0	7.0	
r_{TOT} (mm)		.69	.49	.47	.46	.45	.45	.81	.61	.46	.46	.45	.45	.81	.61	.46	.46	.45	.45	.81	.61	.46	.46	.45	
ΔE_{TOT} (eV)		91	222	517	929	1270	1270	144	352	819	1470	2010	2010	144	352	819	1470	1470	2010	144	352	819	1470	2010	
dE_2 (eV)		.53	.80	1.20	1.60	1.86	1.86	.53	.80	1.20	1.60	1.86	1.86	.53	.80	1.20	1.60	1.60	1.86	.53	.80	1.20	1.60	1.86	
dE_3 (eV)		.18	.44	1.03	1.85	2.53	2.53	.18	.44	1.02	1.83	2.50	2.50	.18	.44	1.02	1.83	1.83	2.50	.18	.44	1.02	1.83	2.50	
dE_{TOT} (eV)		.55	.91	1.58	2.45	3.14	3.14	.55	.91	1.57	2.43	3.12	3.12	.55	.91	1.57	2.43	2.43	3.12	.55	.91	1.57	2.43	3.12	

CRYSTAL		Si (220)						Si (220)						Si (220)						Si (220)					
ENERGY (keV)		4	6	9	12	14	14	4	6	9	12	14	14	4	6	9	12	14	14	4	6	9	12	14	
R (m)		1.24	1.86	2.79	3.72	4.34	4.34	1.24	1.86	2.79	3.72	4.34	4.34	1.24	1.86	2.79	3.72	3.72	4.34	1.24	1.86	2.79	3.72	4.34	
r_{TOT} (mm)		1.10	.73	.51	.40	.35	.35	1.20	.86	.63	.47	.47	.35	1.20	.86	.63	.47	.47	.35	1.20	.86	.63	.47	.47	
ΔE_{TOT} (eV)		38	121	302	555	763	763	60	192	479	879	1208	1208	60	192	479	879	879	1208	60	192	479	879	1208	
dE_1 (eV)		.22	.34	.50	.67	.78	.78	.22	.34	.50	.67	.78	.78	.22	.34	.50	.67	.67	.78	.22	.34	.50	.67	.78	
dE_2 (eV)		.07	.23	.58	1.07	1.48	1.48	.07	.24	.60	1.09	1.50	1.50	.07	.24	.60	1.09	1.09	1.50	.07	.24	.60	1.09	1.50	
dE_{TOT} (eV)		.23	.41	.76	1.26	1.67	1.67	.23	.42	.78	1.28	1.69	1.69	.23	.42	.78	1.28	1.28	1.69	.23	.42	.78	1.28	1.69	

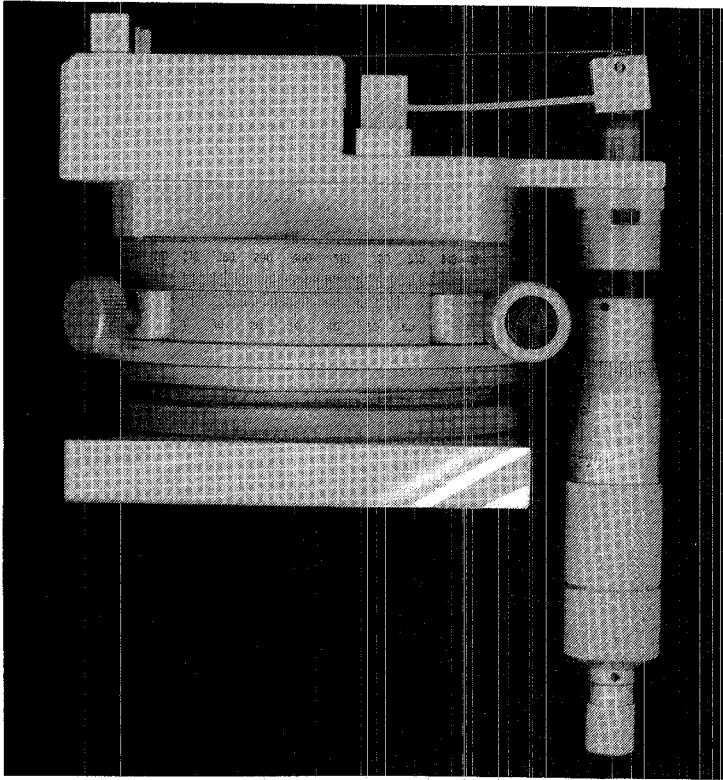


FIG. 6

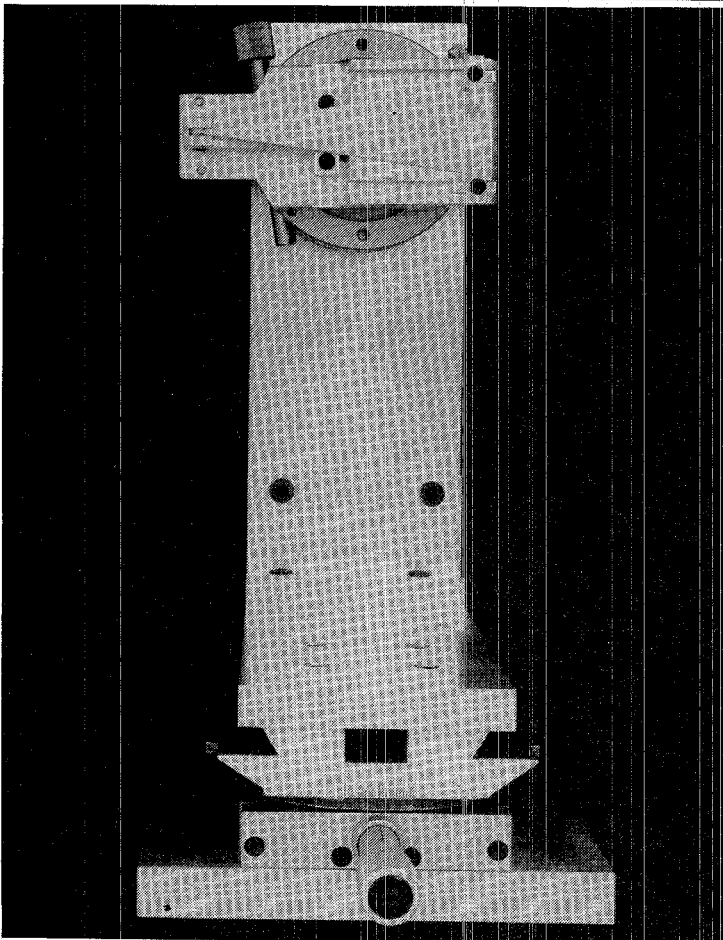


FIG. 7

All the system is set on a $(\Theta, 2\Theta)$ goniometer in order to incline accurately the crystal respect to the beam thus choosing the middle glancing angle Θ_0 , which selects the mean energy of the reflected beam.

Many tests have been performed on such bending crystal holder at the Physics Division of the EURATOM of Ispra, using a conventional X-ray source.

Tests included:

- a) focussing properties;
- b) uniformity of the curvature;
- c) stress of the crystal induced by the holder;
- d) elastic properties of the system.

In order to check the points a,b and c we sent the X-ray beam of a conventional Cu X-ray tube on different areas of the crystal surface observing the focus position and image with X-ray sensitive films and a proportional counter position sensitive detector.

In the ideal case the two characteristic lines $K_{\alpha 1}$ and $K_{\alpha 2}$, which have different energies and so are reflected from different crystal points, must merge at the focus position.

Indeed a crystal stress or non uniformity of the curvature will change the focussing properties along the crystal surface, resulting in a distortion of the K_{α} line profile or in a change of the focus position, when different crystal areas are illuminated.

In spite of this the focus has been found at the right position with no observable distortions.

The elastic response of the crystal has been tested by curving the crystal and measuring the focus position, then leaving the crystal in the bent position for some hours and then measuring again the focus position. After that the crystal has been released and we started again with a new cycle and this for many times.

Also in this case the crystal answer was quite good, confirming that the bending system works very well.

5. - CONCLUSIONS

In this report we have described the first steps done in developing a dispersive EXAFS apparatus to be installed at one of the Frascati S.R. facilities.

We have outlined the theory of the X-ray focussing spectrometer and reported the expected performances of such a spectrometer if used on one of the existing X-ray beam lines. We described also the crystal holder and bender.

The next steps to realise such facility will be:

- 1) test of the bent crystal on the S.R. beam, task which will be performed in the next future;
- 2) choice and test of photodiode arrays or CCD as X-ray position sensitive detectors useful for such measurements.

This second point is much more problematic for the radiation damage suffered by such detectors due to high fluxes X-ray beams.

REFERENCES

- ¹ E. A. Stern, D. E. Sayers and F. W. Lytle, *Phys. Rev. B* 11, 4836 (1975)
- ² P. A. Lee, P. H. Citrin, P. Eisenberger and B. M. Kincaid, *Rev. Mod. Phys.* 53, 769 (1981)
- ³ P. H. Citrin, P. Eisenberger and R. C. Hewit, *Phys. Rev. Lett.* 41, 309 (1978)
- ⁴ J. Stohr, "X-ray Absorption: Principles, Applications, Techniques of EXAFS, SEXAFS and XANES", ed. by R. Prins and D. Koningsberger (Wiley, New York, 1985)
- ⁵ R. P. Phizackerly, Z. U. Rek, G. B. Stephenson, S. D. Conradson, K. O. Hodgson, T. Matsushita and H. Oyanagi, *J. Appl. Cryst.* 16, 220 (1983)
- ⁶ E. Dartyge, C. Depautex, J. M. Dubuisson, A. Fontaine, A. Jucha, P. Leboucher and G. Tourillon, *Nucl. Instr. Meth. A* 246, 452 (1986)
- ⁷ J. Samson, "Techniques of vacuum ultraviolet spectroscopy". J. Wiley and Sons, New York (1967)
- ⁸ Laboratori Nazionali di Frascati - Annual Report 1979 and 1981
- ⁹ E. Burattini, A. Reale, E. Bernieri, N. Cavallo, A. Morone, M. R. Masullo, R. Rinzivillo, G. Dalba, P. Fornasini and C. Mencuccini, *Nucl. Instr. Meth.* 208, 91 (1983)